HHS Public Access

Author manuscript

Acta Biomater. Author manuscript; available in PMC 2018 September 01.

Published in final edited form as:

Acta Biomater. 2017 September 01; 59: 181–191. doi:10.1016/j.actbio.2017.07.005.

Mussel-Inspired PLGA/polydopamine Core-shell Nanoparticle for Light Induced Cancer Thermochemotherapy

Dr Huacheng He[†,‡], **Dr Eleni Markoutsa**[†,‡], **Dr Yihong Zhan**[§], **Dr Jiajia Zhang, PhD**[§] **[Prof]**, and **Dr Peisheng Xu**[†,*] **[Prof]**

[†]Department of Drug Discovery and Biomedical Sciences, College of Pharmacy, University of South Carolina, 715 Sumter St., Columbia, SC 29208, United States

[§]Department of Epidemiology and Biostatistics, University of South Carolina, 800 Sumter Street, Columbia, South Carolina 29208, United States xup@sccp.sc.edu

Abstract

Most photothermal converting systems are not biodegradable, which bring the uneasiness when they are administered into human body due to the uncertainty of their fate. Hereby, we developed a mussel-inspired PLGA/polydopamine core-shell nanoparticle for cancer photothermal and chemotherapy. With the help of an anti-EGFR antibody, the nanoparticle could effectively enter head and neck cancer cells and convert near-infrared light to heat to trigger drug release from PLGA core for chemotherapy as well as ablate tumors by the elevated temperature. Due to the unique nanoparticle concentration dependent peak working-temperature nature, an overheating or overburn situation can be easily prevented. Since the nanoparticle was retained in the tumor tissue and subsequently released its payload inside the cancer cells, no any doxorubicin-associated side effects were detected. Thus, the developed mussel-inspired PLGA/polydopamine core-shell nanoparticle could be a safe and effective tool for the treatment of head and neck cancer.

Graphical abstract

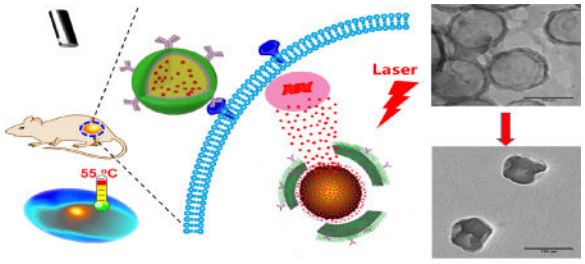

[*]**Corresponding Author**: Author to whom correspondence should be addressed. xup@sccp.sc.edu.

[‡]H. He and E. Markoutsa contributed equally.

Supporting Information Available: Further experimental data regarding the characterization of DOX@PLGA nanoparticle, FACS spectra of SH-SY5Y cells, and blood test results.

Conflict of Interest: The authors declare no competing financial interest.

Keywords

Mussel-inspired; PLGA nanoparticle; thermochemotherapy; EGFR targeted; cancer treatment

1. Introduction

Photothermal therapy (PTT) has been extensively explored for cancer treatment by coupling localized near-infrared (NIR) irradiation and locally accumulated photothermal converting agents (PTCAs) [1]. By far, most developed PTCAs are made of metal based nanostructures, such as gold nanorod, gold nanoshell, gold nanocage, CuSx nanocrystal [2–4]. Due to the localized surface plasmon resonance (LSPR) phenomenon, these nanoparticles generate heat upon light irradiation. By adjusting their size, shape, and geometry, the LSPR peaks of these nanostructures can be tuned to a tissue transparent window (650–900 nm), where light can penetrate deeply [5]. Because of that, upon NIR irradiation, PTCAs generate heat that can be applied for photothermal therapy for cancer and other diseases [5–12]. Due to the slow or nondegradable nature of these metal based PTCAs, they are retained in many organs after finishing their mission. It was found that, for hollow gold nanospheres, about 70% and 95% of them can be retained in the liver and spleen, respectively, 3 months postinjection as compared with their corresponding amounts 1day postinjection [13]. On the contrary, only around 5% and 7% of CuS nanoparticles were retained in the liver and spleen, respectively, 3 months postinjection as compared with their corresponding amounts 1 day postinjection. Furthermore, Guo et al. revealed that there is an irreversible change in the proteomic profile of the liver in mice administered with hollow gold nanospheres, while the change in the proteomic profile of the liver in mice receiving CuS nanoparticles treatment is reversible. Thus, the long-term safety concerns have thwarted the clinical PTT application of gold nanoparticle based PTCAs [14, 15].

Poly(lactic-co-glycolic acid) (PLGA) is a US Food and Drug Administration (FDA) approved biodegradable material, which has been extensively explored as drug carriers for cancer targeted therapy. Since PLGA is not responsive to pH and redox potential, the release of the payload from PLGA based carriers is mainly controlled by the degradation rate of the polymer, depending on its molecular weight and copolymer ratio [16, 17]. To endow light triggerable release capacities to these carriers, PLGA nanoparticles have been coated or embedded with various metal-based PTCAs [18, 19]. However, the inherited non-degradable nature of those PTCAs remains a challenge for their clinical translation.

Epidermal growth factor receptor (EGFR) is overexpressed in many cancer cells including non-small cell lung cancer, colorectal cancer, and head and neck cancer [20]. Cetuximab, a chimeric (mouse/human) monoclonal antibody for EGFR, has been approved by FDA as an EGFR inhibitor for the treatment of colorectal cancer and head and neck cancer [20–22]. Meanwhile, due to its specificity for EGFR overexpressing cancer cells, cetuximab has been explored as a targeting ligand to guide nanocarriers to selectively kill lung cancer cells, glioblastoma cells, and pancreatic cancer cells [23–25].

In nature, mussels powerfully adhere to various surfaces mainly attributes to 3,4-dihydroxyphenyl-l-alanine (DOPA), which contains reactive catechol, and lysine [26].

Inspired by the unique of mussel, Messersmith et al. developed a surface modification technology with dopamine, which contains catecholamine functional groups [27]. In weak basic environment, dopamine can be self-polymerized to form a polydopamine (PD) layer on the surface of numerous materials. Furthermore, the newly formed PD layer can subsequently react with thiol or amine containing biomolecules to yield surface functionalized materials [27–29]. In addition, researchers found that PD nanoparticle has a strong absorbance in the NIR region and can generate heat upon NIR irradiation [30]. PD coated manganese oxide nanoparticles and Fe_3O_4 nanoparticle have been explored for the treatment of cancer by photothermal therapy [31, 32]. Hereby, we developed a photothermal converting nanomaterial based on the core/shell structure of biodegradable PLGA and polydopamine (Figure 1A). To be more effective in killing cancer cells, doxorubicin (DOX) was encapsulated into the cetuximab functionalized nanoparticle. We expect that NIR irradiation can induce photothermal effect, and subsequently trigger the release of the encapsulated DOX to exhibit both photothermal therapy and chemotherapy for head and neck cancer (Figure 1B). In addition, different from CuS_x nanoparticles, the proposed system does not involve the copper homeostasis to control its systemic toxicity.

2. Materials and Methods

2.1. Chemicals

Poly(lactic-co-glycolic acid) (PLGA, 50/50, 16 kDa) was purchased from Lakeshore Biomaterials, Inc. (Birmingham, AL, USA). Polyvinyl alcohol (PVA, Mw=9,000–10,000 Da), (3-(4,5-dimethylthiazol-2-yl)-2,5-diphenyltetrazolium bromide (MTT), Poly(ethylene glycol) methyl ether thiol (PEG-SH, Mn= 2,000 Da), Propidium Iodide (PI), Dopamine hydrochloride were purchased from Sigma-Aldrich Chemical Co. (St. Louis, MO, USA). Penicillin (10,000 U/mL), streptomycin (10,000 mg/mL), 0.25% trypsin-EDTA, Dulbecco's Modified Eagle Medium (with L-glutamine) and fetal bovine serum (FBS) were obtained from American Type Culture Collection (ATCC, Manassas, VA, USA). Doxorubicin (DOX) was purchased from AK Scientific, Inc. (Union City, CA, USA). Cetuximab was acquired from ImClone LLC (Princeton, NJ, USA). Calcein AM was purchased from Thermo Fisher Scientific, Inc. (Waltham, MA, USA).

2.2. DOX@PLGA Nanoparticle Fabrication

DOX encapsulated PLGA nanoparticle was fabricated by emulsion method [33]. In brief, 5 mg DOX was first dissolved in 1 mL CH_3OH with 25 μL triethylamine and mixed with 5 mL CH_2Cl_2 containing 200 mg PLGA. The mixture solution was then poured into 20 mL 5% PVA solution on ice, followed by ultrasonication for 15 min (Misonix Sonicator, XL-2015, 80% power). After sonication, the emulsion solution was added into 100 mL ddH_2O and stirred overnight to evaporate the organic solvent. The DOX@PLGA nanoparticle was centrifuged at 1000 g for 10 min to remove big aggregates and then centrifuged at 16000 g for 15 min to collect the particles. The particles were washed with ddH_2O three times via a Millipore Stirred Ultrafiltration Cell (MWCO: 10,000 Da) to remove excess PVA and non-encapsulated DOX and redispersed in 10 mL ddH_2O and kept at 4 °C for further use.

2.3. Dopamine Coating

The coating of dopamine onto the surface of DOX@PLGA nanoparticles was according to a previously reported method [34]. Briefly, 6 mg DOX@PLGA nanoparticles were redispersed in 12 mL tris buffer (10 mM, pH 8.5) with 6 mg dopamine. The mixture was kept stirring for 3 h at room temperature in an opened glass vial. The solution turned its color from yellowish brown to dark brown, indicating the successful coating of polydopamine on the DOX@PLGA nanoparticle. Finally, the DOX@PLGA/PD nanoparticle was collected by centrifuging at 16000 g for 10 min and washed for three times and redispersed in 6 mL tris buffer (20 mM, pH 8.5) for the subsequent surface modification.

2.4. PEG and Anti-EGFR Antibody Decoration

DOX@PLGA/PD nanoparticle suspension (2 mL) prepared above was mixed with 4 mg thio-PEG2000 and 4 mg Anti-EGFR antibody (cetuximab) in 2 mL PBS buffer (pH 7.4), respectively, and stirred for 30 min. The pH of the mixture was immediately adjusted to 7.0 by adding 1N HCl. The PEG and EGFR antibody decorated nanoparticles were collected by centrifuging at 16000 g for 10 min at 4 °C and washed 2 times to yield DOX@PLGA/PD-PEG and DOX@PLGA/PD-C. The resulting nanoparticles were redispersed in 500 μL ddH_2O or DMEM culture medium and stored at 4 °C. The supernatant of cetuximab decorated nanoparticle was collected and the unconjugated anti-EGFR antibody was quantified by Bio-Rad assay. It was found that the cetuximab conjugation efficiency was 59.6%.

2.5. Nanoparticle Characterization

The DOX concentration in the nano-suspension was determined by measuring the fluorescence intensity (Ex=485 nm, Em=595 nm) after dissolving nanoparticles in DMSO and calculated according to pre-known calibration curve. The UV-Vis spectrum of DOX@PLGA nanoparticle before and after dopamine coating was recorded. To quantify the loading efficiency and content, nanoparticles were freeze dried to get the weight amounts. The morphology of DOX@PLGA, DOX@PLGA/PD, and DOX@PLGA/PD-C were observed by TEM and the hydrodynamic size and zeta potential of nanoparticles were measured by DLS. For DLS measurement, nanoparticles were dispersed in 1 mM PBS 7.4 (0.2 mg/mL). The glass transition temperatures of the nanoparticles were measured by differential scanning calorimetry (Q2000, TA Instruments, heated from 25 °C to 80 °C with a heat flow rate of 1 °C/min).

2.6. Serum Stability

To investigate the serum stability, DOX@PLGA, DOX@PLGA/PD-PEG, and DOX@PLGA/PD-C were diluted with 10% FCS (equivalent DOX concentration was 15 μg/mL) and incubated at 37 °C up for 7 days. The sizes of the nanoparticles were monitored by DLS.

2.7. Photothermal Conversion and Efficiency Calculation

To test the photothermal effect of DOX@PLGA/PD-PEG nanoparticles, 50 μL nanoparticles with OD values equal to 0.15, 0.375, 0.75, 1.2, 1.875, and 3.75 were irradiated with a 808

nm NIR laser (2.83 W/cm^2, Scorpius-D IR Portable Laser, Laserglow Technologies) for 10 min. The temperatures of the nanoparticles were recorded every 1 min by FLIR thermal camera (FLIR i7, FLIR ® Systems, Inc.). For photothermal conversion efficiency measurement, DOX@PLGA/PD -PEG nanoparticle (50 μL, OD value equal to 0.75) was irradiated at 808 nm for 9 min and the temperature was recorded every 10 sec. After that, the laser was removed and the decreasing of the temperature of the nanoparticle was continued to be monitored every 10 s till 9 min. Finally, the photothermal conversion efficiency was calculated according to previous report.[27] The photothermal conversion efficiency of DOX@PLGA/PD-PEG ( ) was 16.9%.

2.8. In vitro DOX Release

The release profile of DOX from nanoparticles was measured at pH 5.0 and pH 7.4 with or without laser irradiation. In brief, DOX@PLGA/PD-PEG nanoparticle was centrifuged and re-dispersed in 500 μL acetate buffer (10 mM, pH 5.0) and PBS buffer (10 mM, pH7.4), respectively, and incubated at 37 °C. Both buffers were supplemented with 2% Tween 80 to create a sink condition by improving the solubility of DOX. The initial DOX concentration in the suspension was 20 μg/mL. Each pH group included six parallel samples. At predetermined time points, all samples were centrifuged at 16,000 g for 10 min. After that, 250 μL supernatants were carefully retrieved and refilled with 250 μL fresh buffers to redisperse the nanoparticles. At 24 h and 32 h post incubation, three samples in each pH group were irradiated with 808 nm laser for 10 min while the other three samples were kept at 37 °C. All samples were continuously incubated up to 72 h. After that, the releasing of DOX from the nanoparticles were quantified by a microplate reader (Ex=495 nm, Em=595 nm, Beckman Coulter DTX 880 Multimode Detector, Beckman Coulter, Inc.).

2.9. Confocal Microscopy

Human head and neck squamous carcinoma cell line, UMSCC 22A, was a gift from Dr. Anna-Liisa Nieminen (Medical University of South Carolina). Cells were cultured in Dulbecco's modified Eagle's medium (DMEM) (Invitrogen) supplemented with 10% fetal bovine serum (FBS) and penicillin/streptomycin (complete culture medium) in a humidified incubator at 37 °C with 5% CO2, 95% air. UMSCC 22A cells (200,000cells/dish) were seeded in 35mm^2 Petri dishes (Mat Tek, MA, USA) overnight. After that, DOX, DOX@PLGA/PD-PEG, and DOX@PLGA/PD-C nanoparticles were added into the cells at the DOX equivalent concentration of 2 μg/mL. In order to study the effect of free anti-EGFR antibody on the uptake of DOX@PLGA/PD-C nanoparticle, cells were pretreated with free anti-EGFR antibody (200 μg/mL) for 30 min before adding the nanoparticles. Cells were then incubated at 37 °C for 3 h. After that, cells were washed with PBS (3×), fixed with formaldehyde (4.5 % in PBS), and stained with Hoechst 33342 (final concentration 1μg/mL). Cells were analyzed under a confocal microscope (LSM 700, Carl-Zeiss Inc.).

2.10. Flow Cytometry

UMSCC 22A cells (300,000cells/well) were seeded in 6-well plates overnight. After that, DOX, DOX@PLGA/PD-PEG, and DOX@PLGA/PD-C nanoparticles were added at the DOX equivalent concentration of 1 μg/mL. In order to investigate the effect of EGFR on the cellular uptake of DOX@PLGA/PD-C nanoparticle, cells were pretreated with free anti-

EGFR antibody (200 μg/mL) 30 min before adding DOX@PLGA/PD-C nanoparticles. The plate was incubated at 37 °C for 3 h. Then cells were washed, trypsinized and resuspended in PBS. DOX-positive cell population was quantified at Ex=488 nm, Em=585 nm using flow cytometry (BD Accuri C6, BD Biosciences). As a negative control, the cellular uptake of different nanoparaticles in SH-SY5Y cell (obtained from ATCC), an EGFR negative cell line, was also tested.

2.11. Live & Dead Cell Assay

To study the photothermal cytotoxicity of the nanoparticles, Live and Dead cell assay was introduced. In brief, UMSCC 22A cells (300,000 cells/well) were seeded in 6-well plates and incubated under a humidified atmosphere of 95/5% air/CO_2 until 100% confluency. Then free DOX, PLGA/PD-PEG, DOX@PLGA/PD-PEG, and DOX@PLGA/PD-C were added to the plates. The equivalent DOX concentration was 10 μg/mL and the absorbances at 808 nm for all nanoparticles were kept the same. Cells were incubated at 37 °C for another 2 h and exposed to the 808 nm NIR laser for 30 min. Here we used longer irradiation time compared to the irradiation time in MTT assay because we wanted to make sure that obvious photothermal cytotoxicity could be observed immediately after laser irradiation. After that, cells were gently washed with PBS (2×) to avoid washing off dead cells. Calcein AM (0.2 μM) and propidium iodide (PI, 25 μg/mL) mixture solution (500 μL) was added and kept at room temperature for 30 min and then cells were observed directly by fluorescence microscopy (Olympus IX81, Olympus America Inc.).

2.12. In vitro Cytotoxicity

The cytotoxicity of nanoparticles was evaluated by MTT assay. UMSCC 22A cells were seeded in a 96-well plate (20,000 cells/well) for 24 prior to the study. Then free DOX, DOX@PLGA/PD-PEG, and DOX@PLGA/PD-C with DOX concentration equivalent to 2, 5 and 10 μg/mL were added. The cells were then incubated in 95/5% air/CO_2 at 37 °C for 3 h, followed by the irradiation of the 808 nm laser for 10 min. After that, all wells were washed 2 times and replaced with fresh culture medium and kept incubated for another 24 h. Finally, MTT reagent (100 μL, 5 mg/mL) in medium) was added and incubated for 4h, following the addition of MTT stop solution and the measurement of the optical density of the medium using a microplate reader (ELX808, Bio-Tech Instrument, Inc) at = 595 nm.

2.13. Tumor Growth Inhibitory Assay

All animal experiments were conducted in accordance with NIH regulations and approved by the Institutional Animal Care and Use Committee of the University of South Carolina. UMSCC 22A cells (3×10^6 cells in 100 μL DMEM medium) were inoculated subcutaneously in female Balb/c nude mice (8–10 week old, ~20 g, Jackson Laboratory). The tumor volume was measured by a digital caliper and calculated according to the following formula: Tumor volume = (tumor length) × (tumor width)^2/2. When the tumor reached to 50 mm^3, free DOX and DOX@PLGA/PD-C were intratumorally injected (40 μL, DOX concentration equivalent to 15 μg/mL). For the control group, PBS was injected. Mice were exposed to an 808 nm laser irradiation (2.83 W/cm^2) 3 h post injection for 10 min. The temperature of the mice during the irradiation was recorded by the FLIR thermal camera. The tumor volumes (V) of the mice were measured every other day for 24 days. The relative tumor volume expressed

as V/V_0 (V_0 was the tumor volume when the treatment was initiated) was used to represent the tumor size change during the whole treatment process. After 24 days, the mice were sacrificed and the blood, tumor, liver, heart, lung, kidneys, and spleen were collected for further analysis. All organs were firstly fixed in 10% neutral buffered formalin for 24 h and then washed with PBS and finally kept in 70% ethanol at 4 °C.

2.14. Blood Analysis

Whole blood samples (50 μL) of the mice were firstly collected in heparinized tubes and analyzed with VetScan HM5 (Abaxis, Inc.) for white blood cells, red blood cells, neutrophils, etc.

2.15. TEM Analysis for Heart Tissue

To study the cardiotoxicity of DOX, the hearts of the mice were analyzed by TEM. The formalin fixed samples were further fixed with 1% perosmic oxide for 2 h at 4 °C, washed with water and then dehydrated in a series of alcohol solutions, embedded, and sliced with the thickness between 50 and 70 nm. TEM analysis was performed on Hitachi H8000 operating at 200 kV.

2.16. Histological Examinations

The formalin fixed organs were embedded in OCT gel, sectioned into ~5 μm, stained with hematoxylin and eosin (H&E) and analyzed by light microscopy (Leica DM1000 LED, Leica Microsystems Inc.). The histology was performed in a blinded fashion by professional personnel at the University of South Carolina.

2.17. Statistical Analysis

The results were reported as the mean•±•standard deviation of three different studies. ANOVA analysis was carried out to determine statistical significance ($p•<•0.05$) of the experimental data.

3. Results and Discussion

3.1. Fabrication and Characterization of DOX-Loaded Polydopamine Coated PLGA Nanoparticle

The DOX-loaded PLGA nanoparticle (DOX@PLGA) was fabricated according to our published emulsion method [33], and then coated with PD under the weak basic condition as shown in Figure 1A. The dark rings in Figure1E and F proved the formation of a PD layer on the PLGA shell, which is about 13.4 nm. The feeding ratio for DOX/PLGA was 2.5% (5 mg DOX/200 mg PLGA). The final loading content for DOX@PLGA and DOX@PLGA/PD were 1.82% and 1.38%, respectively. The approach used to collect nanoparticle was centrifugation, which is not an efficient approach. To improve the prodctivity and yield, one potential alternative is using Millipore Amicon™ Ultra-15 Centrifugal Filter Unit to collect these nanoparticles. To enhance the stability and cancer cell targeting effect of the DOX@PLGA/PD nanoparticles, polyethylene glycol (PEG) and anti-EGFR antibody (cetuximab) were conjugated onto the surface of the polydopamine (PD) (Figure 1A),

respectively. Dynamic light scattering (DLS) found that the size of DOX@PLGA was about 110 nm (Figure 2A). The coating of PD layer increased the size of DOX@PLGA/PD to 135 nm. The addition of PEG protection layer and cetuximab slightly increased the size of DOX@PLGA/PD-C nanoparticles to 142 nm, which coincided with the observation of TEM (Figure 1). Zetasizer found that DOX@PLGA/PD-C carried a negative surface charge (−14. 6± 0.5 mV). Polymerized dopamine has been reported to bind on solid surfaces via covalent and noncovalent interactions [35]. Due to the lack of thiol groups and amine groups on the surface of PLGA particle, we postulate that the interaction between polydopamine and PLGA nanoparticle is through hydrophobic interaction. The thiol-PEG bind to the polydopamine coated PLGA nanoparticles through the catechols reacting with thiols via Michael addition reaction [27]. The antibody bind to the polydopamine coated PLGA nanoparticles through the catechols reacting with amines via Schiff base reaction. To evaluate the stability of DOX@PLGA/PD-C nanoparticle during blood circulation, the size of the nanoparticle in 10% serum containing medium was monitored with DLS. Due to the existence of a PEG protection layer and negative surface charge, DOX@PLGA/PD-C was stable in culture medium containing 10% FCS (Figure 2B), and no obvious size change and aggregation were observed after one week of incubation.

PLGA nanoparticle has a little absorption in the NIR region, while PD has been reported showing strong absorbance in that window. After the coating of polydopamine, the absorption of PLGA/PD nanoparticle increased in the NIR region (Figure 2C). Differential scanning calorimetry (DSC) revealed that PD coating significantly increased the glass transition temperatures (Tg) of PLGA nanoparticle from 39.42 to 42.97 °C (Figure 2D), suggesting that PLGA/PD nanoparticle could be a temperature sensitive carrier for targeted drug delivery.

3.2. Photothermal Concerting Property of PLGA/PD Nanoparticle

It has been reported that polydopamine nanoparticle can generate heat upon NIR irradiation [30]. The coating of PD on the surface of PLGA nanoparticle boosted its absorbance in the NIR region (Figure 2C). Our control experiment proved that PLGA nanoparticle itself could not produce heat upon NIR irradiation (Figure S1). To evaluate whether this increased absorbance in NIR region would endow PLGA/PD with the ability to generate enough heat to elevate the solution temperature, the PLGA/PD nano-suspensions of different concentrations were irradiated with NIR laser (808 nm, 2.83 W/cm^2) for 10 min at predesigned time intervals and their temperatures were monitored with an FLIR i7 thermal imaging camera and recorded every 30 sec. Figure 3A revealed that PLGA/PD could effectively heat the media and exhibited a concentration-dependent photothermal effect. At the OD of 0.75, PLGA/PD nanoparticle quickly heated the solution temperature to 45 °C, indicating that PLGA/PD is a good photothermal converting material. Based on the heating and cooling cycle shown in Figure 3B, we found the photothermal converting efficiency of PLGA/PD is 16.9%, which is lower than that of gold nanorod (~22%,),[22] a widely used nanomaterial for cancer therapy. Interestingly, for those experiments, medium temperature reached higher than 60 °C, we also noticed that medium temperature quickly reached its summit within 3 minutes and then exhibited as a plateau (Figure 3A). This phenomenon was not observed for most developed photothermal converting materials, since their media

temperatures always raise when the NIR irradiation is applied [36–39]. This unique dose dependent-peak temperature feature could be critical for photothermal therapy, during which burning adjacent healthy tissue should be avoided. To observe the morphology change after the NIR irradiation, we further examined DOX@PLGA/PD nanoparticles with TEM. Compared with the structure shown in Figure 1F, the size of the particles shrank after irradiation (Figure 1H). Furthermore, the original core/shell structure was clearly compromised, indicating the breakage of the PD shell. We postulate that contraction of the particle size was due to the melting of the nanoparticle above Tg during the heating process, while the breakage of the PD shell was caused by the heterogeneous heat stress responses between the PLGA core and PD shell.

3.3. Drug Release Kinetic of DOX@PLGA/PD Nanoparticle

To investigate whether the coating of PD on the surface of PLGA nanoparticle could affect the release profile of its payload, anticancer drug doxorubicin (DOX) was adopted as a model drug. Subcellular colocalization study validated that both DOX@PLGA and DOX@PLGA/PD-C nanoparticles enter UMSCC 22A through endosome-lysosome pathway (Figure S2). DOX@PLGA/PD nanoparticle was suspended in sodium acetate buffer (pH 5.0) and phosphate buffer (PBS, pH 7.4) to mimic the environments in the lysosome and cytosol, respectively. Figure 3C showed that DOX@PLGA/PD released 40.85% and 57.63% of its payload within 24 h of incubation in PBS and sodium acetate buffer, respectively. As we already proved PLGA/PD nanoparticle could efficiently convert NIR laser irradiation into heat, we further investigated the effect of NIR irradiation on DOX release kinetics. Remarkably, Figure 3C showed that the two pulses of 10 min of NIR irradiations induced 30% more DOX release for both pH conditions.

3.4. Live and Dead Cell Assay

To investigate the cell killing effect of NIR irradiation coupled with DOX@PLGA/PD on the head and neck cancer cells, live and dead cell assay was carried out immediately after the irradiation. As we expected, for cells co-incubated with PLGA/PD nanoparticle, nearly all non-irradiated cells were green (Figure 3D), while NIR irradiated cells were red. The distinct irradiation boundary as shown in red/green in the well treated with PLGA/PD nanoparticle and NIR irradiation suggests that NIR irradiation induced photothermal effect could effectively kill cancer cells while PLGA/PD nanoparticle itself is non-toxic. Due to the relatively short incubation time, most cells treated with DOX were alive. Therefore, no significant difference was observed between the cells treated with DOX@PLGA/PD and PLGA/PD.

3.5. EGFR Targeting Effect on Cellular Uptake

Epidermal growth factor receptor (EGFR) is overexpressed in many types of cancer, including colon cancer, lung cancer, glioblastoma multiforme, and head and neck cancer [20]. To enhance cellular uptake of DOX@PLGA/PD nanoparticles for UMSCC 22A head and neck cancer cells, an anti-EGFR antibody, cetuximab, was conjugated onto the surface of the particle. Confocal microscopy found that more red fluorescence signals were observed in cells treated with cetuximab conjugated DOX@PLGA/PD-C than its non-targeted counterpart (Figure 4A). In addition, the pre-treatment of free cetuximab significantly

decreased the uptake of DOX@PLGA/PD-C nanoparticles, which proves the EGFR mediated endocytosis. The EGFR mediated cellular uptake of DOX@PLGA/PD-C nanoparticles and the blocking effect of free cetuximab were also observed by flow cytometry (Figure 4B). It is worthy to mention that free DOX entered cancer cells faster than the DOX@PLGA/PD-C nanoparticles (Figure 4B). Flow cytometry experiment was also carried out to study the cellular uptake of DOX@PLGA/PD-C in SH-SY5Y cell, an EGFR negative cell line, and compared it with that of DOX@PLGA/PD. The result in Figure S3 revealed that there is no difference between the EGFR targeted and non-targeted nanoparticle in entering SH-SY5Y, indicating that EGFR targeted nanoparticle couldn't boost the uptake by EGFR-negative cells. Combining the data shown in Figure 4B, we can conclude that DOX@PLGA/PD-C selectively enhances the uptake of EGFR positive cancer cells.

3.6. Cell Killing Effect of DOX@PLGA/PD-C Nanoparticle Coupled with NIR Irradiation

To investigate whether the enhanced cellular uptake of DOX@PLGA/PD-C nanoparticles and photothermal effect of the nanoparticle can be translated into higher efficacy in killing cancer cells, cell proliferation assay was employed. Figure 4C revealed that empty PLGA/PD nanoparticles are almost non-toxic, while effectively killing cancer cells when coupled with NIR irradiation at the concentration corresponding to 10 μM DOX. It is worth noting that the effect of NIR irradiation only became significant when PLGA/PD nanoparticles were added at the DOX corresponding of 5 μM or higher, at which PLGA/PD could generate enough heat to ablate cancer cells and augment drug release. The EGFR targeted nanoparticles showed much higher efficacy in killing UMSCC 22A cells than their non-targeted counterparts. As expected, NIR irradiation significantly boosted the cytotixic potency of DOX@PLGA/PD and DOX@PLGA/PD-C, which reflects the combination effect of photothermal effect and its subsequent induced quicker drug release. Free DOX exhibited higher cell killing effect than other treatments except at 10 μM dose.

3.7. Tumor Growth Inhibitory Effect of DOX@PLGA/PD-C Nanoparticle Coupled with NIR Irradiation

To investigate the tumor growth inhibitory effect of EGFR targeted DOX@PLGA/PD coupled with NIR irradiation, a subcutaneous head and neck cancer mouse model was introduced. Since intratumoral injection is a widely-adopted route of administration in clinic for treating head and neck cancer patient [40–43], to maximize the therapeutic effect of the treatment, free DOX, PLGA/PD-C, DOX@PLGA/PD, and DOX@PLGA/PD-C nanoparticles were administered intratumorally. The thermal images shown in Figure 5A indicated that EGFR targeted PLGA/PD could quickly elevate the temperature of tumor tissue to 55 °C within 2 min. For most developed photothermal systems, the temperature of their treated tissues continuously increases when NIR irradiation is turned on [44–47]. Interestingly, as shown in the nano-suspension, the PLGA/PD system treated tissue maintained its temperature constantly at 55 °C during the whole course of NIR irradiation. The tumor mass in the DOX@PLGA/PD-C coupled with NIR irradiation treatment group collapsed and formed a scar 2 days post treatment (Figure 5E). The scar gradually faded away and the original tumor did not recur during a 24-day period (Figure 5B and E). Contrary to its strong potency shown in the *in vitro* study, free DOX treatment initially only

slightly reduced tumor size when compared with its original size (Figure 5B and D). Furthermore, those tumors gradually bounced back 10 days post treatment. As expected, the non-treated tumors grew to 10 times of its initial size at the end of the experiment (Figure 5B). Comparing the tumor growth rates between DOX@PLGA/PD and DOX@PLGA/PD-C treated groups, we found that the addition of cetuximab did enhanced the efficacy of DOX loaded nanoparticles (Figure 5B). Therefore, cetuximab is required to boost the effect of photothermal and chemotherapy. In addition, the treatment of PLGA/PD-C+ NIR, which includes both the effect of NIR and EGFR targeting, was far less effective as compared with DOX@PLGA/PD-C + NIR. Thus, the combination of NIR, DOX and cetuximab is required to achieve the best anticancer effect. The negligible tumor mass in Figure 5B and **5E** proved that DOX@PLGA/PD-C coupled with NIR irradiation is an effective approach for eradicating head and neck tumor. We did not observe significant body weight change in all groups (Figure 5C).

3.8. Tissue Histology and Cardiotoxicity Assay

Cardiotoxicity is a major side effect associated with DOX based chemotherapy [48–50]. To evaluate the safety of DOX@PLGA/PD-C coupled with NIR irradiation, hearts in the treated groups were collected and processed for TEM observation [51]. TEM image (top panel of Figure 6) revealed that the membrane integrity and ordered structure of mitochondria in the heart tissue of the mice receiving free DOX treatment have been significantly compromised. To our surprise, no abnormal structure was observed in the heart tissue of mice treated with DOX@PLGA/PD-C coupled with NIR irradiation. Furthermore, no histopathological changes were observed in the liver tissues among all treatment groups. Similarly, blood components analysis did not detect significant alteration among all treatment groups (Table S1). In addition, H&E staining of the tumor tissue (low panel of Figure 6) showed that the control and DOX-treated tumor kept the characteristics of squamous cell carcinoma, while the apoptosis-related shrunk nuclei in the DOX@PLGA/PD-C coupled with NIR irradiation treated tumor proved its effectiveness. All these results indicate that DOX@PLGA/PD-C coupled with NIR irradiation is a safe tool for head and neck cancer therapy.

5. Conclusions

In summary, a doxorubicin loaded biodegradable photothermal converting material based on a mussel inspired PLGA/polydopamine core/shell nano-structure has been developed for cancer photothermal therapy and chemotherapy. With the help of the anti-EGFR antibody, the nanoparticle could effectively enter head and neck cancer cells and convert near-infrared light to heat to trigger drug release from the PLGA core for chemotherapy as well as ablate tumors by the elevated temperature. Due to the unique PLGA/PD concentration dependent peak working temperature nature, an overheating or overburn situation can be easily prevented. Since the nanoparticle was retained in the tumor tissue and subsequently released its payload inside the cancer cells, an doxorubicin-associated cardio-toxicity was mimimized. Owing to its unique biodegradable feature, the DOX@PLGA/PD-C nanoparticle could be a promising tool for head and neck cancer treatment.

Supplementary Material

Refer to Web version on PubMed Central for supplementary material.

Acknowledgments

The authors want to thank the ASPIRE award from the Office of the Vice President for Research of The University of South Carolina and National Institutes of Health (5P20GM109091-02 and 1R15CA188847-01A1) for financial support of the research. We also want to thank Dr. Chuangbin Tang for the DSC measurement.

References

1. Khan MS, Vishakante GD, Siddaramaiah H. Gold nanoparticles: A paradigm shift in biomedical applications. Adv. Colloid Interface Sci. 2013; 199:44–58. [PubMed: 23871224]
2. Liu XS, Huang N, Li H, Wang HB, Jin Q, Ji J. Multidentate Polyethylene Glycol Modified Gold Nanorods for in Vivo Near-Infrared Photothermal Cancer Therapy. ACS Appl. Mater. Interfaces. 2014; 6(8):5657–5668. [PubMed: 24673744]
3. Chen J, Wiley B, Li ZY, Campbell D, Saeki F, Cang H, Au L, Lee J, Li X, Xia Y. Gold Nanocages: Engineering Their Structure for Biomedical Applications. Adv. Mater. 2005; 17(18):2255–2261.
4. Wang SH, Riedinger A, Li HB, Fu CH, Liu HY, Li LL, Liu TL, Tan LF, Barthel MJ, Pugliese G, De Donato F, D'Abbusco MS, Meng XW, Manna L, Meng H, Pellegrino T. Plasmonic Copper Sulfide Nanocrystals Exhibiting Near-Infrared Photothermal and Photodynamic Therapeutic Effects. ACS nano. 2015; 9(2):1788–1800. [PubMed: 25603353]
5. Alkilany AM, Thompson LB, Boulos SP, Sisco PN, Murphy CJ. Gold nanorods: their potential for photothermal therapeutics and drug delivery, tempered by the complexity of their biological interactions. Adv. Drug Deliv. Rev. 2012; 64(2):190–9. [PubMed: 21397647]
6. Kwon KC, Ryu JH, Lee JH, Lee EJ, Kwon IC, Kim K, Lee J. Proteinticle/Gold Core/Shell Nanoparticles for Targeted Cancer Therapy without Nanotoxicity. Adv. Mater. 2014; 26(37):6436–41. [PubMed: 25044204]
7. Zhang Z, Wang J, Chen C. Near-infrared light-mediated nanoplatforms for cancer thermo-chemotherapy and optical imaging. Adv. Mater. 2013; 25(28):3869–80. [PubMed: 24048973]
8. Skrabalak SE, Chen J, Au L, Lu X, Li X, Xia Y. Gold Nanocages for Biomedical Applications. Adv. Mater. 2007; 19(20):3177–3184. [PubMed: 18648528]
9. Dong W, Li Y, Niu D, Ma Z, Gu J, Chen Y, Zhao W, Liu X, Liu C, Shi J. Facile synthesis of monodisperse superparamagnetic Fe3O4 Core@hybrid@Au shell nanocomposite for bimodal imaging and photothermal therapy. Adv. Mater. 2011; 23(45):5392–7. [PubMed: 21997882]
10. Yavuz MS, Cheng Y, Chen J, Cobley CM, Zhang Q, Rycenga M, Xie J, Kim C, Song KH, Schwartz AG, Wang LV, Xia Y. Gold nanocages covered by smart polymers for controlled release with near-infrared light. Nat. Mater. 2009; 8(12):935–9. [PubMed: 19881498]
11. Dickerson EB, Dreaden EC, Huang X, El-Sayed IH, Chu H, Pushpanketh S, McDonald JF, El-Sayed MA. Gold nanorod assisted near-infrared plasmonic photothermal therapy (PPTT) of squamous cell carcinoma in mice. Cancer Lett. 2008; 269(1):57–66. [PubMed: 18541363]
12. Loo C, Lin A, Hirsch L, Lee MH, Barton J, Halas N, West J, Drezek R. Nanoshell-enabled photonics-based imaging and therapy of cancer. Technol. Cancer Res. Treat. 2004; 3(1):33–40. [PubMed: 14750891]
13. Guo L, Panderi I, Yan DD, Szulak K, Li Y, Chen YT, Ma H, Niesen DB, Seeram N, Ahmed A, Yan B, Pantazatos D, Lu W. A comparative study of hollow copper sulfide nanoparticles and hollow gold nanospheres on degradability and toxicity. ACS nano. 2013; 7(10):8780–93. [PubMed: 24053214]
14. Khlebtsov N, Dykman L. Biodistribution and toxicity of engineered gold nanoparticles: a review of in vitro and in vivo studies. Chem. Soc. Rev. 2011; 40(3):1647–1671. [PubMed: 21082078]
15. Fraga S, Brandao A, Soares ME, Morais T, Duarte JA, Pereira L, Soares L, Neves C, Pereira E, Bastos MD, Carmo H. Short- and long-term distribution and toxicity of gold nanoparticles in the

rat after a single-dose intravenous administration. Nanomedicine. 2014; 10(8):1757–1766. [PubMed: 24941462]

16. Sun B, Ranganathan B, Feng SS. Multifunctional poly(D,L-lactide-co-glycolide)/montmorillonite (PLGA/MMT) nanoparticles decorated by Trastuzumab for targeted chemotherapy of breast cancer. Biomaterials. 2008; 29(4):475–486. [PubMed: 17953985]
17. Zhang ZP, Lee SH, Feng SS. Folate-decorated poly(lactide-co-glycolide)-vitamin E TPGS nanoparticles for targeted drug delivery. Biomaterials. 2007; 28(10):1889–1899. [PubMed: 17197019]
18. Fazio E, Scala A, Grimato S, Ridolfo A, Grassi G, Neri F. Laser light triggered smart release of silibinin from a PEGylated-PLGA gold nanocomposite. J. Mater. Chem. B. 2015; 3(46):9023–9032.
19. Song JB, Yang XY, Jacobson O, Huang P, Sun XL, Lin LS, Yan XF, Niu G, Ma QJ, Chen X. Ultrasmall Gold Nanorod Vesicles with Enhanced Tumor Accumulation and Fast Excretion from the Body for Cancer Therapy. Adv. Mater. 2015; 27(33):4910–4917. [PubMed: 26198622]
20. Yewale C, Baradia D, Vhora I, Patil S, Misra A. Epidermal growth factor receptor targeting in cancer: A review of trends and strategies. Biomaterials. 2013; 34(34):8690–8707. [PubMed: 23953842]
21. Yarom N, Jonker DJ. The role of the epidermal growth factor receptor in the mechanism and treatment of colorectal cancer. Discov. Med. 2011; 11(57):95–105. [PubMed: 21356164]
22. Grande R, Gemma D, Sperduti I, Gelibter A, Giampaolo MA, Trombetta G, Nelli F, Gamucci T. Changing monoclonal antibody keeping unaltered the chemotherapy regimen in metastatic colorectal cancer patients: is efficacy maintained? SpringerPlus. 2013; 2(1):185. [PubMed: 23667824]
23. Wang Y, Huang HY, Yang L, Zhang Z, Ji H. Cetuximab-modified mesoporous silica nano-medicine specifically targets EGFR-mutant lung cancer and overcomes drug resistance. Sci. Rep. 2016; 6:25468. [PubMed: 27151505]
24. Mortensen JH, Jeppesen M, Pilgaard L, Agger R, Duroux M, Zachar V, Moos T. Targeted antiepidermal growth factor receptor (cetuximab) immunoliposomes enhance cellular uptake in vitro and exhibit increased accumulation in an intracranial model of glioblastoma multiforme. J. Drug Deliv. 2013; 2013:209205. [PubMed: 24175095]
25. Khan JA, Kudgus RA, Szabolcs A, Dutta S, Wang E, Cao S, Curran GL, Shah V, Curley S, Mukhopadhyay D, Robertson JD, Bhattacharya R, Mukherjee P. Designing nanoconjugates to effectively target pancreatic cancer cells in vitro and in vivo. PloS one. 2011; 6(6):e20347. [PubMed: 21738572]
26. Zhao H, Waite JH. Linking adhesive and structural proteins in the attachment plaque of Mytilus californianus. J. Bio.Chem. 2006; 281(36):26150–8. [PubMed: 16844688]
27. Lee H, Dellatore SM, Miller WM, Messersmith PB. Mussel-inspired surface chemistry for multifunctional coatings. Science. 2007; 318(5849):426–430. [PubMed: 17947576]
28. Liu YL, Ai KL, Lu LH. Polydopamine Its Derivative Materials: Synthesis Promising Applications in Energy, Environmentaland Biomedical Fields. Chem. Rev. 2014; 114(9):5057–5115. [PubMed: 24517847]
29. Ye Q, Zhou F, Liu WM. Bioinspired catecholic chemistry for surface modification. Chem. Soc. Rev. 2011; 40(7):4244–4258. [PubMed: 21603689]
30. Liu YL, Ai KL, Liu JH, Deng M, He YY, Lu LH. Dopamine-Melanin Colloidal Nanospheres: An Efficient Near-Infrared Photothermal Therapeutic Agent for In Vivo Cancer Therapy. Adv. Mater. 2013; 25(9):1353–1359. [PubMed: 23280690]
31. Mu X, Zhang F, Kong C, Zhang H, Zhang W, Ge R, Liu Y, Jiang J. EGFR-targeted delivery of DOX-loaded Fe3O4@ polydopamine multifunctional nanocomposites for MRI and antitumor chemo-photothermal therapy. Int. J. Nanomedicine. 2017; 12:2899–2911. [PubMed: 28435266]
32. Ding X, Liu J, Li J, Wang F, Wang Y, Song S, Zhang H. Polydopamine coated manganese oxide nanoparticles with ultrahigh relaxivity as nanotheranostic agents for magnetic resonance imaging guided synergetic chemo-/photothermal therapy. Chem. Sci. 2016; 7(11):6695–6700. [PubMed: 28451112]

33. Xu P, Gullotti E, Tong L, Highley CB, Errabelli DR, Hasan T, Cheng JX, Kohane DS, Yeo Y. Intracellular drug delivery by poly(lactic-co-glycolic acid) nanoparticles revisited. Mol. Pharm. 2009; 6(1):190–201. [PubMed: 19035785]
34. Park J, Brust TF, Lee HJ, Lee SC, Watts VJ, Yeo Y. Polydopamine-Based Simple and Versatile Surface Modification of Polymeric Nano Drug Carriers. ACS nano. 2014; 8(4):3347–3356. [PubMed: 24628245]
35. Lee H, Scherer NF, Messersmith PB. Single-molecule mechanics of mussel adhesion. Proc. Natl. Acad. Sci. U S A. 2006; 103(35):12999–3003. [PubMed: 16920796]
36. Yang J, Lee J, Kang J, Oh SJ, Ko HJ, Son JH, Lee K, Suh JS, Huh YM, Haam S. Smart Drug-Loaded Polymer Gold Nanoshells for Systemic and Localized Therapy of Human Epithelial Cancer. Adv. Mater. 2009; 21(43):4339-+. [PubMed: 26042940]
37. Wang XY, Zhang JS, Wang YT, Wang CP, Xiao JR, Zhang Q, Cheng YY. Multi-responsive photothermal-chemotherapy with drug-loaded melanin-like nanoparticles for synergetic tumor ablation. Biomaterials. 2016; 81:114–124. [PubMed: 26731575]
38. Cheng B, He H, Huang T, Berr SS, He J, Fan D, Zhang J, Xu P. Gold Nanosphere Gated Mesoporous Silica Nanoparticle Responsive to Near-Infrared Light and Redox Potential as a Theranostic Platform for Cancer Therapy. J.Biomed.Nanotech. 2016; 12(3):435–449.
39. Lin L-S, Yang X, Niu G, Song J, Yang H-H, Chen X. Dual-enhanced photothermal conversion properties of reduced graphene oxide-coated gold superparticles for light-triggered acoustic and thermal theranostics. Nanoscale. 2016; 8(4):2116–2122. [PubMed: 26726809]
40. Wenig BL, Werner JA, Castro DJ, Sridhar KS, Garewal HS, Kehrl W, Pluzanska A, Arndt O, Costantino PD, Mills GM, Dunphy FR 2nd, Orenberg EK, Leavitt RD. The role of intratumoral therapy with cisplatin/epinephrine injectable gel in the management of advanced squamous cell carcinoma of the head and neck. Arch. Otolaryngol. Head Neck Surg. 2002; 128(8):880–5. [PubMed: 12162764]
41. Villaret D, Glisson B, Kenady D, Hanna E, Carey M, Gleich L, Yoo GH, Futran N, Hung MC, Anklesaria P, Heald AE. A multicenter phase II study of tgDCC-E1A for the intratumoral treatment of patients with recurrent head and neck squamous cell carcinoma. Head Neck. 2002; 24(7):661–9. [PubMed: 12112540]
42. Castro DJ, Sridhar KS, Garewal HS, Mills GM, Wenig BL, Dunphy FR 2nd, Costantino PD, Leavitt RD, Stewart ME, Orenberg EK. Intratumoral cisplatin/epinephrine gel in advanced head and neck cancer: a multicenter, randomized, double-blind, phase III study in North America. Head Neck. 2003; 25(9):717–31. [PubMed: 12953307]
43. Fujimoto Y, Mizuno T, Sugiura S, Goshima F, Kohno S, Nakashima T, Nishiyama Y. Intratumoral injection of herpes simplex virus HF10 in recurrent head and neck squamous cell carcinoma. Acta Otolaryngol. 2006; 126(10):1115–7. [PubMed: 16923721]
44. Song X, Gong H, Yin S, Cheng L, Wang C, Li Z, Li Y, Wang X, Liu G, Liu Z. Ultra-Small Iron Oxide Doped Polypyrrole Nanoparticles for In Vivo Multimodal Imaging Guided Photothermal Therapy. Adv. Funct. Mater. 2014; 24(9):1194–1201.
45. Li Z, Huang H, Tang S, Li Y, Yu X-F, Wang H, Li P, Sun Z, Zhang H, Liu C, Chu PK. Small gold nanorods laden macrophages for enhanced tumor coverage in photothermal therapy. Biomaterials. 2016; 74:144–154. [PubMed: 26454052]
46. Piao J-G, Wang L, Gao F, You Y-Z, Xiong Y, Yang L. Erythrocyte Membrane Is an Alternative Coating to Polyethylene Glycol for Prolonging the Circulation Lifetime of Gold Nanocages for Photothermal Therapy. ACS nano. 2014; 8(10):10414–10425. [PubMed: 25286086]
47. Bi H, Dai Y, Lv R, Zhong C, He F, Gai S, Gulzar A, Yang G, Yang P. Doxorubicin-conjugated CuS nanoparticles for efficient synergistic therapy triggered by near-infrared light. Dalton Trans. 2016; 45(12):5101–5110. [PubMed: 26883928]
48. Chatterjee K, Zhang JQ, Honbo N, Karliner JS. Doxorubicin Cardiomyopathy. Cardiology. 2010; 115(2):155–162. [PubMed: 20016174]
49. Miyata M, Suzuki S, Misaka T, Takeishi Y. Senescence Marker Protein 30 has a Cardio-protective Role in Doxorubicin-induced Cardiac Dysfunction. PLoS One. 2013; 8:e79093. [PubMed: 24391705]

50. Al-Harthi SE, Alarabi OM, Ramadan WS, Alaama MN, Al-Kreathy HM, Damanhouri ZA, Khan LM, Osman AMM. Amelioration of doxorubicin-induced cardiotoxicity by resveratrol. Mol. Med. Rep. 2014; 10(3):1455–1460. [PubMed: 25059399]

51. Ma H, Jones KR, Guo R, Xu P, Shen Y, Ren J. Cisplatin Compromises Myocardial Contractile Function and Mitochondrial Ultrastructure: Role of Endoplasmic Reticulum Stress. Clin. Exp. Pharmacol. Physiol. 2010; 37:460–465. [PubMed: 19878217]

The described EGFR targeted PLGA/polydopamine Core-shell Nanoparticle (**PLGA/PD NP**) is novel in the following aspects

- Different from most photothermal converting nanomaterials, PLGA/PD NP is **biodegradable**, which **eliminates the long-term safety concerns** thwarting the clinical application of photothermal therapy.
- Different from most photothermal nanomaterials, upon NIR irradiation, PLGA/PD NP quickly heats its surrounding environment to a NP concentration dependent peak working temperature and **uniquely keeps that temperature constant** through the duration of light irradiation. Due to this unique property an **overheating or overburn situation for the adjacent healthy tissue can be easily avoided**.
- The PLGA/PD NP **releases its payload through detaching PD shell** under NIR laser irradiation.
- The EGFR-targeted doxorubicin-loaded PLGA/PD NP **effectively eradicate head and neck tumor** *in vivo* through the synergism of photothermal therapy and chemotherapy while **not introducing doxorubicin associated cardiotoxicity**.

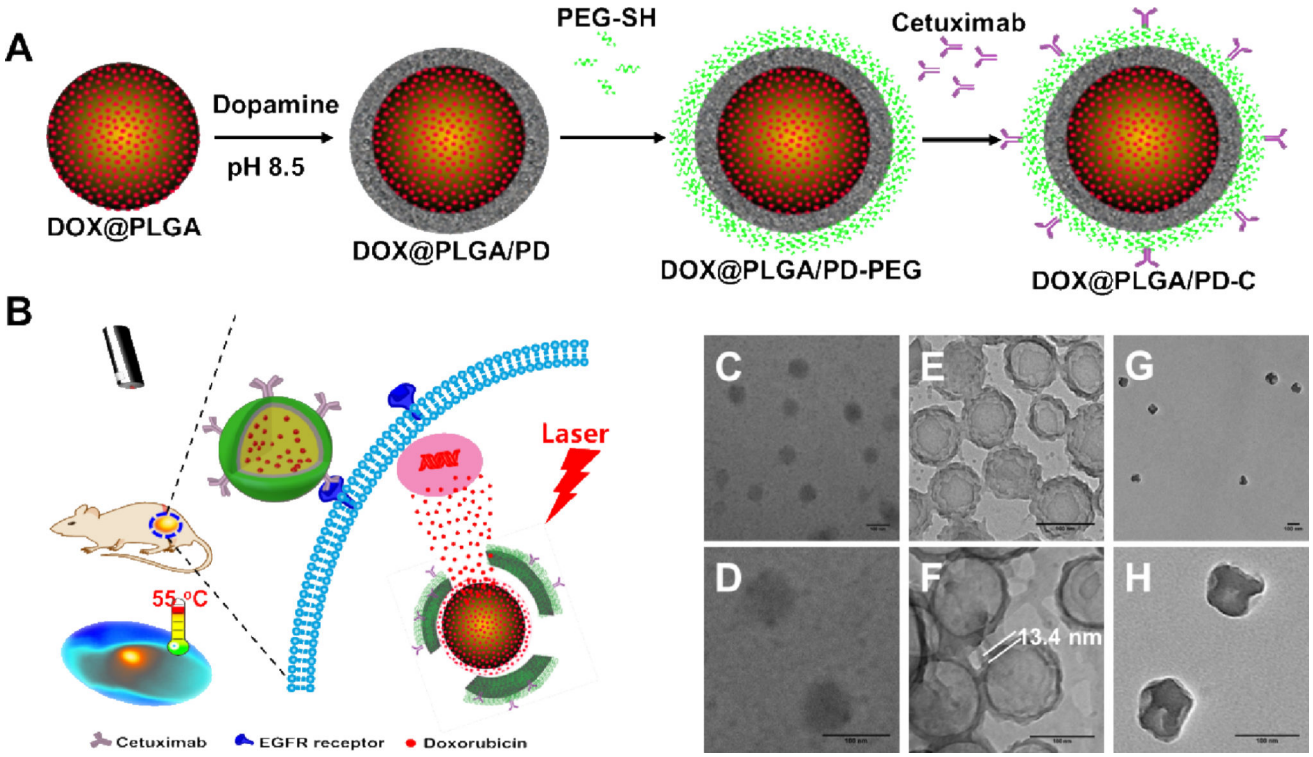

Figure 1.

Schematic illustration of the fabrication of epidermal growth factor receptor targeted mussel inspired nanoparticle (A), and its proposed action pathway (B). TEM images of DOX@PLGA (C–D), DOX@PLGA/PD (E–F), and DOX@PLGA/PD after NIR irradiation (G–H). Scale bars are 100 nm in (C–H).

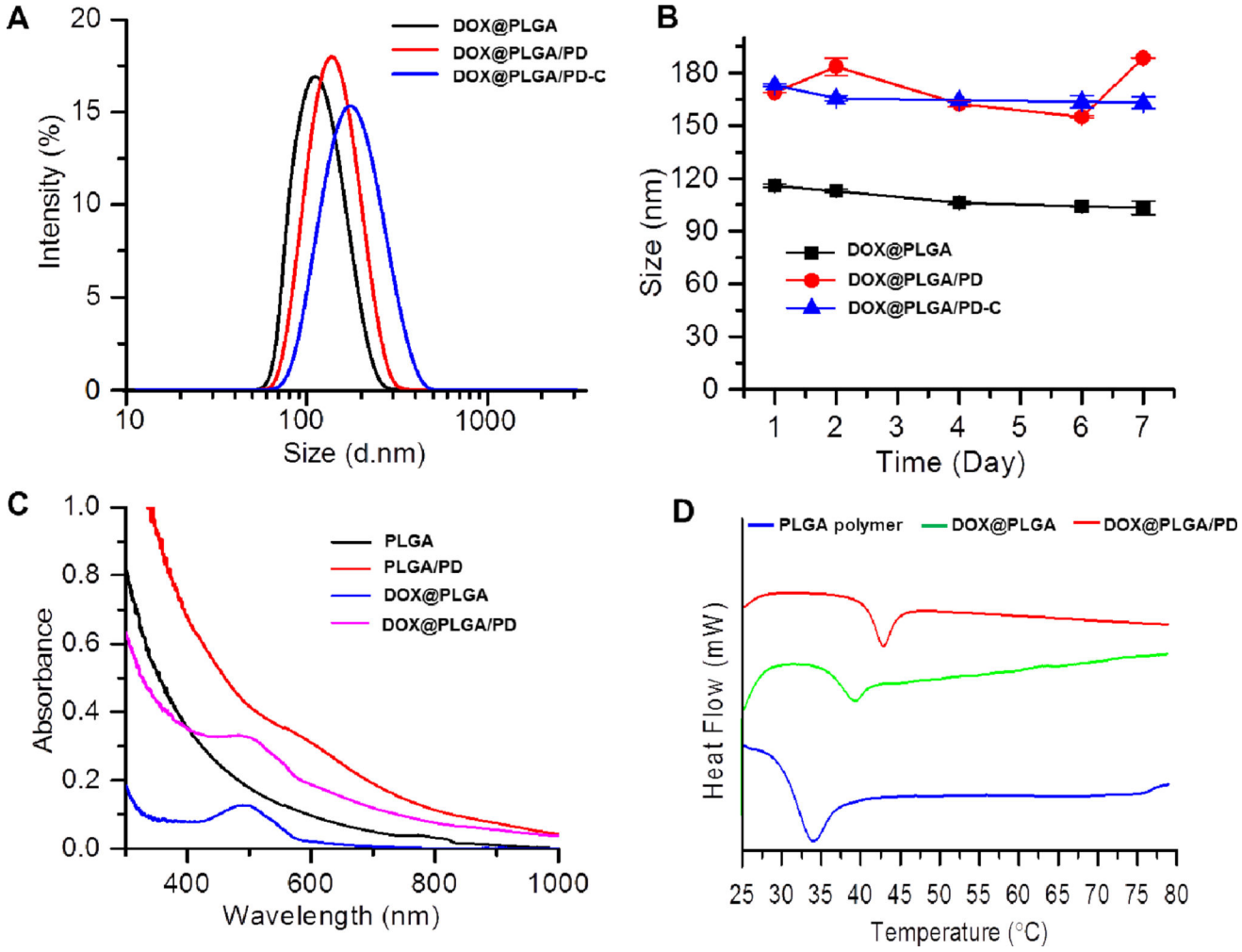

Figure 2.

Physical properties of nanoparticles fabricated based on PLGA polymer. (A) The hydrodynamic size distributions of DOX@PLGA, DOX@PLGA/PD, and DOX@PLGA/PD-C. (B) Serum stability of DOX@PLGA, DOX@PLGA/PD, and DOX@PLGA/PD-C. Nanoparticles were dissolved in 10% FCS and incubated at 37 °C for 7 days. (C) UV-Vis absorption spectra of PLGA, PLDA/PD, DOX@PLGA, and DOX@PLGA/PD. (D) The glass transition temperatures (Tg) of PLGA polymer, DOX@PLGA and DOX@PLGA/PD measured by DSC.

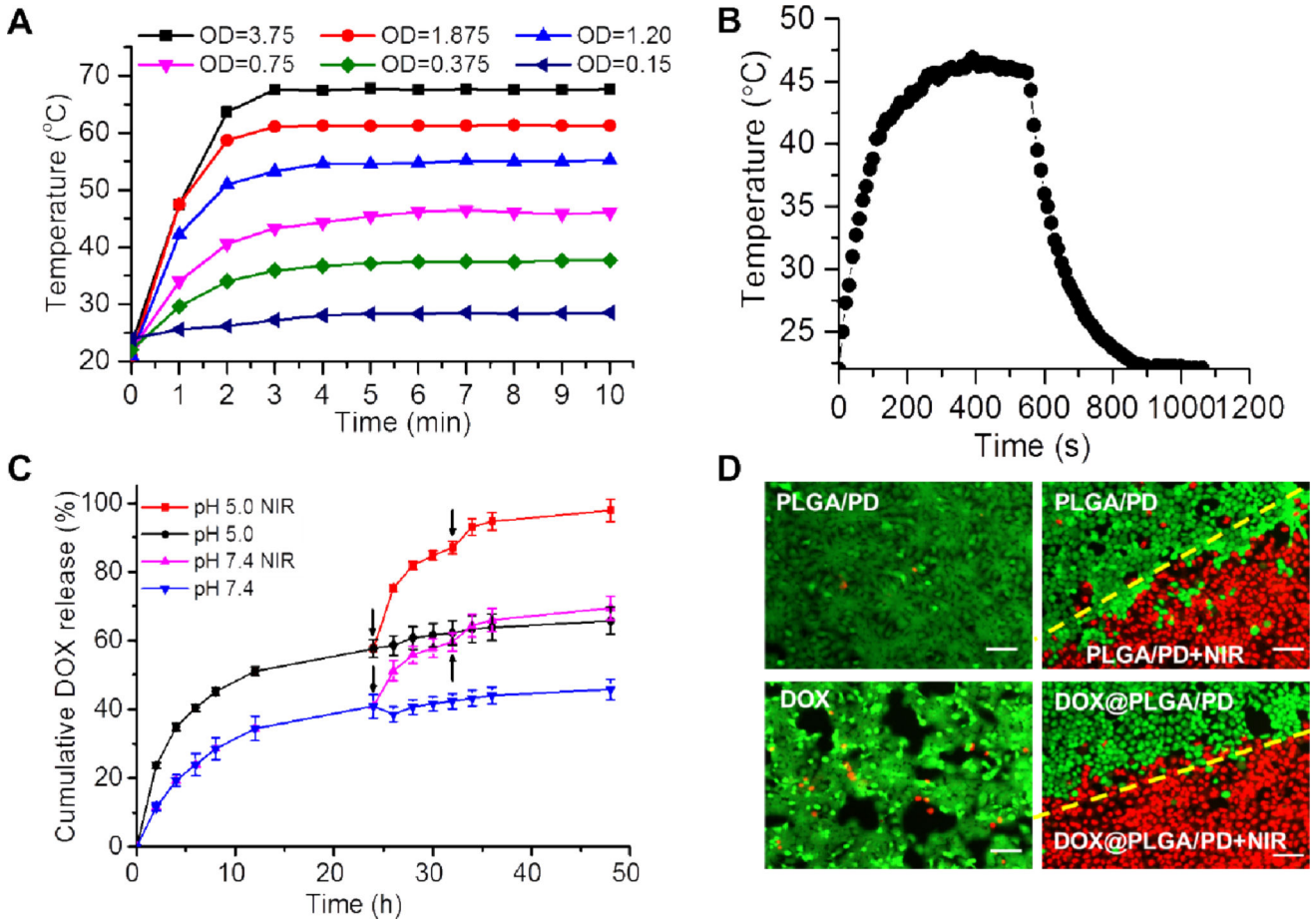

Figure 3.

The photothermal effect of DOX@PLGA/PD on medium temperature elevation (A, B), drug release kinetics (C), and cell viability detected by live/dead cell staining (D). OD represents the absorbance of DOX@PLGA/PD at 808 nm (A). The temperature change of DOX@PLGA/PD nano-suspensions during 1 cycle of NIR irradiation and cooling (B). Arrows indicate the application of NIR irradiation in (C). Images were taken immediately after laser irradiation (D). Scale bars in (D) are 100 μm.

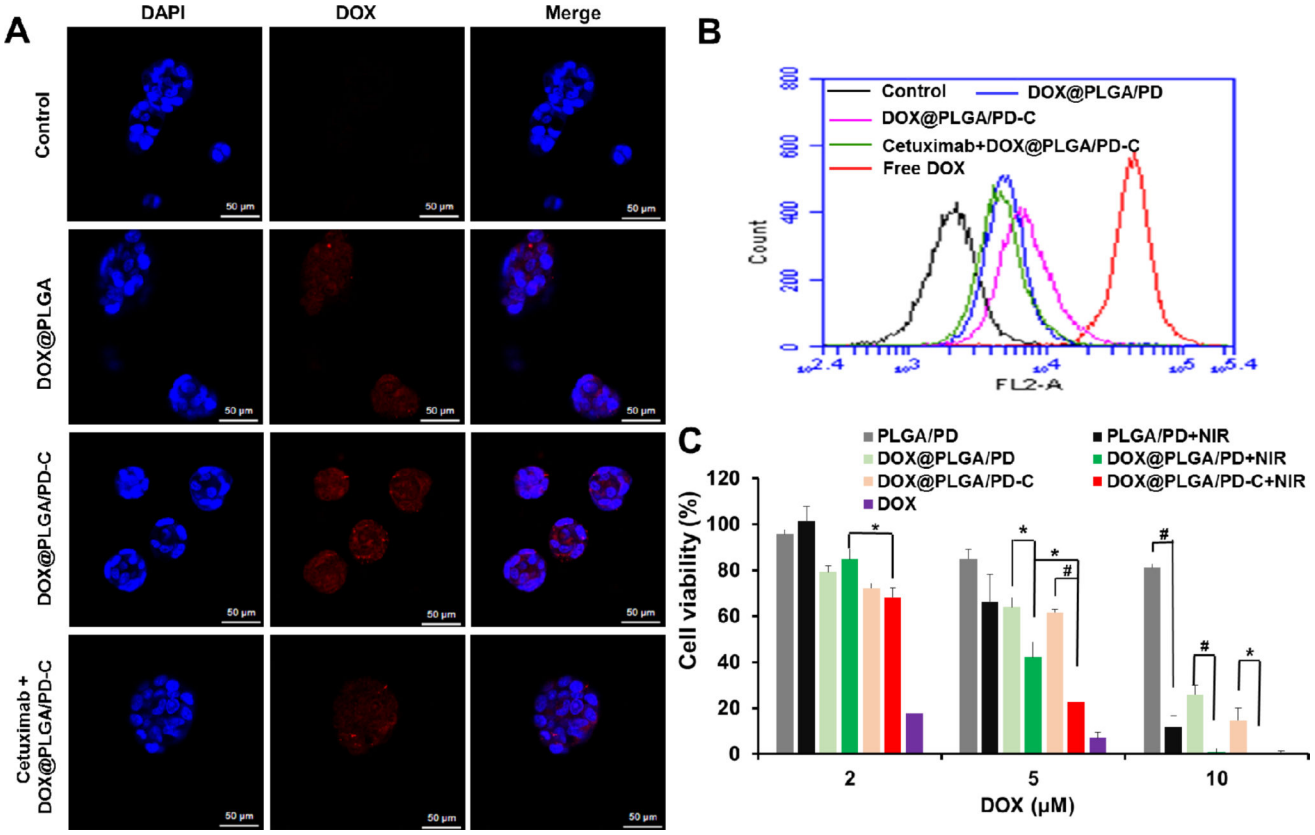

Figure 4.

Confocal images (A), flow cytometry spectra (B), and cytotoxicity (C) of UMSCC 22A cells treated with different conditions. All scale bars in (A) are50 μm. Cells were co incubated with various nanoparticles for 3 h before the confocal observation in (A). Cells received NIR irradiation for 10 min, 2.83 W/cm^2. MTT assay was carried out 24 h after the treatments (C). Data expressed as mean ± SD (ANOVA analysis *$P < 0.05$; #$P < 0.01$).

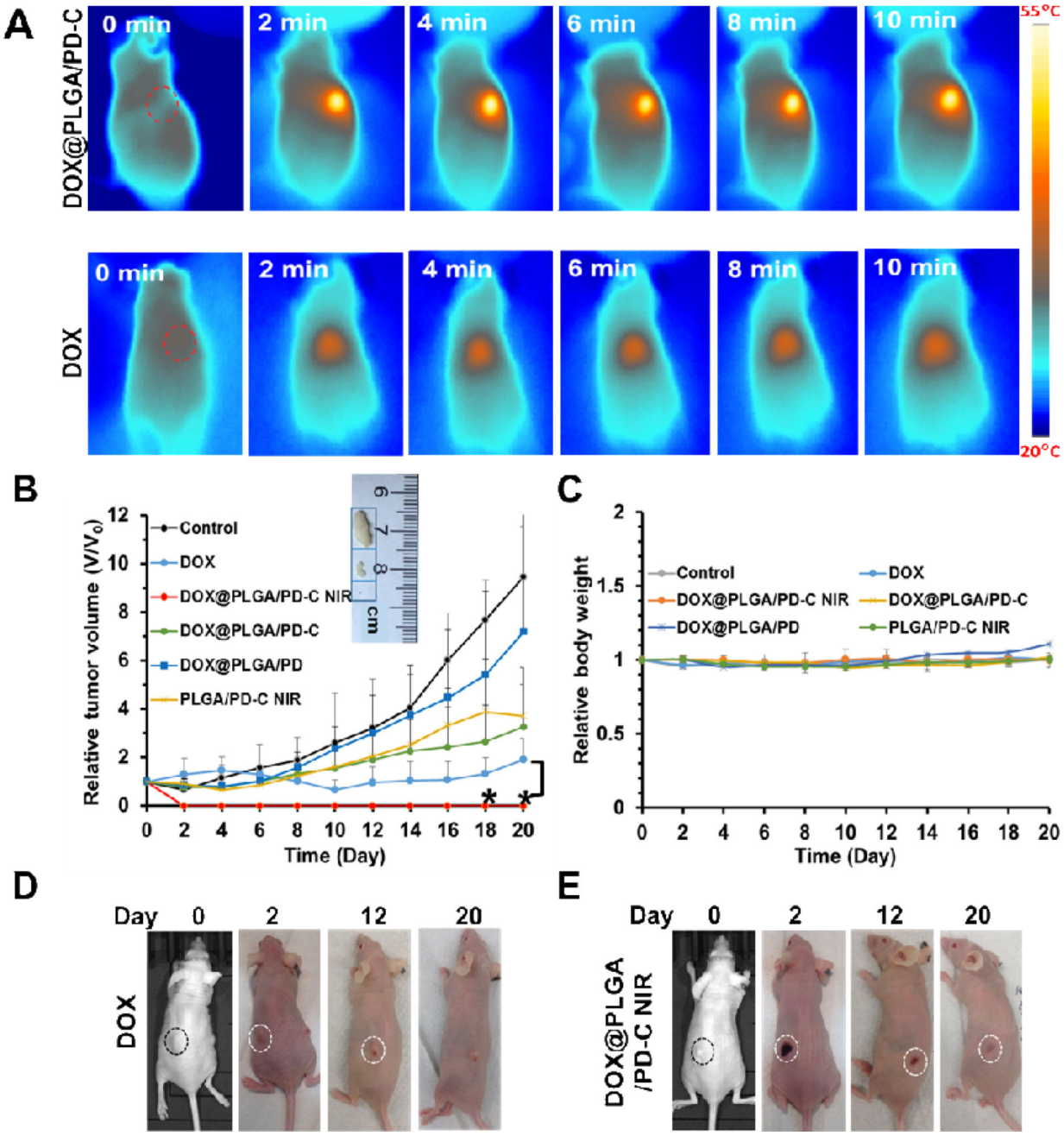

Figure 5.

Tumor response after receiving different treatments. The tumor model was established by s.c. injection of UMSCC 22A cells in the flanks of mice. (A) Thermal image of mice after receiving NIR irradiation over 10 min (2.83 W/cm^2). (B) The tumor volume change profiles of mice after receiving different treatments. Insert shows the representative images of tumors harvested from different treatment groups at the end of the experiment. Data were expressed as mean ± SD (DOX@PLGA/PD-C NIR vs DOX, *$P < 0.05$). (C) The body weight curves of tumor-bearing mice after receiving different treatments. (D) Representative images of developed tumors after receiving DOX treatment. (E) Representative images of developed

tumors after receiving DOX@PLGA/PD-C NIR treatment. Circles in (D) and (E) indicate the location of the tumor.

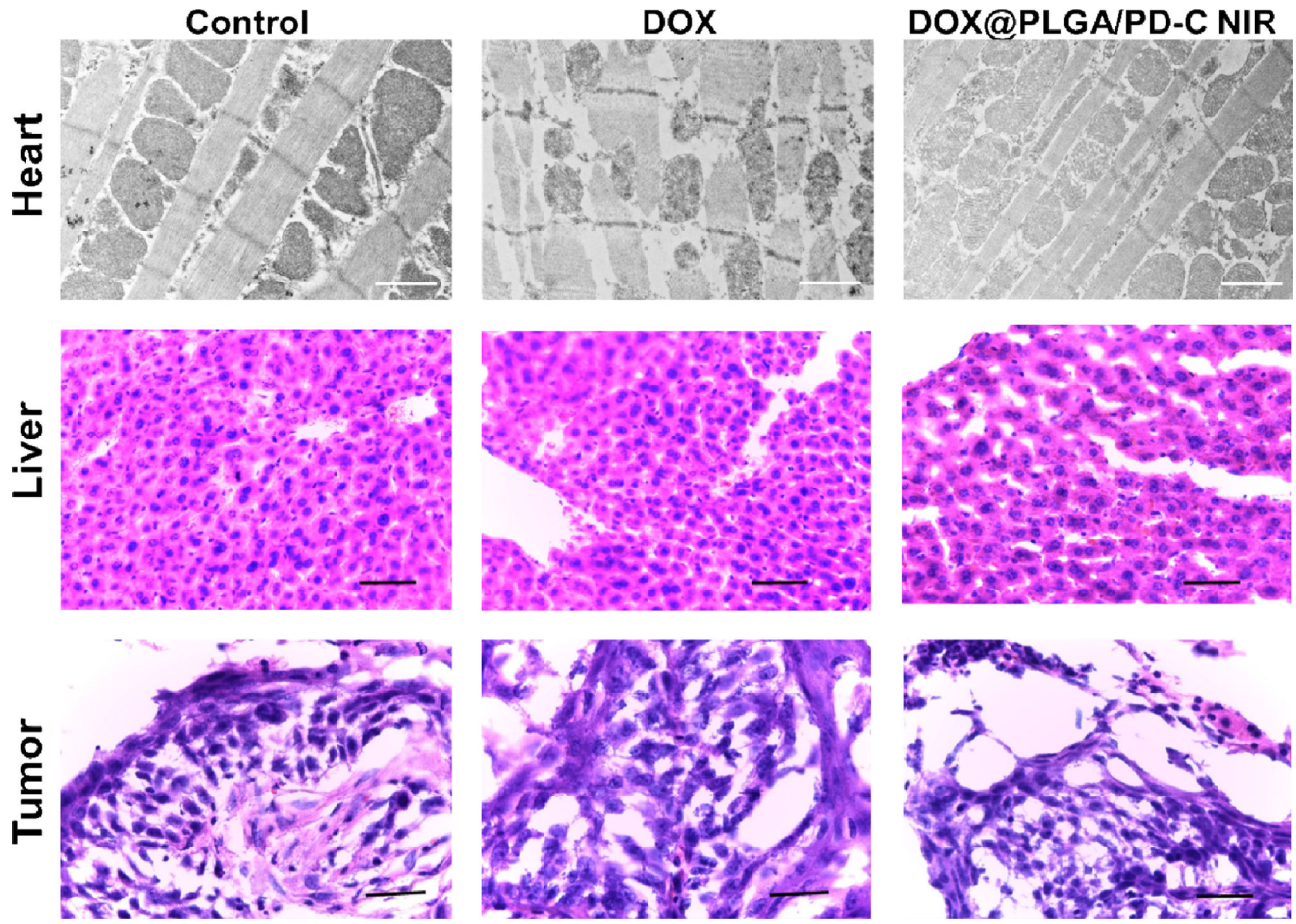

Figure 6.

The TEM images of heart tissue sections and H&E staining images of liver and tumor tissue sections. Scale bars in the TEM images (top panel) and H&E staining sections (middle and bottom panels) are 1 μm and 50 μm, respectively.